

PREDICTING SHORELINE RESPONSE TO CHANGES IN LONGSHORE SEDIMENT TRANSPORT FOR THE RIO GRANDE DO SUL COASTLINE

WILLIAMS, J.J. & ESTEVES, L.S.

School of Geography, University of Plymouth Drake Circus, Plymouth, UK, PL4 8AA

jon.j.williams@plymouth.ac.uk

ABSTRACT

Williams, J.J. & Esteves, L.S. 2006. Predicting shoreline response to changes in longshore sediment transport for the Rio Grande do Sul coastline. Braz. J. Aquat. Sci. Technol. 10(1):1-9. ISSN 1808-7035. Longshore sediment transport (LST) has been calculated using the GERC formula for the long (618 km), gently undulating, sandy shore of Rio Grande do Sul (RS) for wave climate scenarios typifying *normal* (i.e. non-ENSO years) and *La Niña* years. Predicted LST values have been validated with available field measurements. Whilst in most cases LST was directed to the north, simulations revealed large spatial variability in both the magnitude and direction of the net annual LST flux. This was related primarily to the orientation of the coastline relative to the incident waves and to the dominance of waves from different directions. Predicted net annual LST values were used in a simple model to calculate changes in the position of the shoreline. For *normal* years, results showed that areas of erosion predicted along the southern shores of the coastal projections and regions of accretion predicted in the embayments agreed well with shoreline surveys. The wavelength and amplitude of temporal and spatial oscillations in shoreline position measured by DGPS surveys were estimated well by a simple simulation of shoreline change. The simulation showed also that observed reversals in shoreline displacement from erosion to accretion or *vice-versa* could be explained by subtle changes in the annual wave climate. The present results provide strong evidence that slight changes to the wave climate can impact significantly on coastal processes along the RS shoreline. Similar impacts might be anticipated along other sandy shorelines worldwide.

Keywords: Longshore transport, modeling, shoreline changes

INTRODUCTION

Longshore sediment transport, LST, is driven by shore-parallel currents arising from the many interacting processes associated with breaking waves in the surf zone. Most models used to estimate LST make simple assumptions about hydrodynamics and sediment transport and ignore factors such as barred topography and/or cross-shore exchanges. For this reason, measured and predicted LST rates differ between factors of 10 to 100. Although all the models assume that the beach is long and straight and sediment transport is driven only by waves, there are few locations where this is the case.

Following on from the work of Lima *et al.* (2001), the main focus of this paper concerns estimation of the net annual LST rates and accompanying annual changes in shoreline position along the 618 km-long shoreline of Rio Grande do Sul (RS), southern Brazil. This shoreline is largely undeveloped, dominated by waves and for the most part homogeneous with respect to sediments and beach characteristics. Only limited information is available related to the beach profile, LST direction, inter-annual and seasonal changes in the shoreline position, shoreline response to ENSO events, wave breaker height

and direction, and beach slopes below the low water line. However, these data allow simple simulation studies of net LST and associated beach width changes on seasonal and annual time scales. Here the primary objective is to demonstrate that subtle changes in the wave climate can reverse the local shoreline movement from erosion to accretion and *vice-versa*. The present results therefore reveal a mechanism to explain semi-rhythmic seasonal and/or annual changes in shoreline position observed along the RS shoreline and at other locations worldwide.

Study Area

The 618 km of the coastline of RS stretches northwards from approximately 34° to 29° south (Figure 1). The shoreline is characterised by a gently undulating barrier orientated approximately NE-SW with dissipative to intermediate beaches composed of fine sand. The Tramandaí and the Patos lagoon inlets are the only discontinuities in this coastline (Figure 1). Whilst the mean semidiurnal tidal range is only 0.5 m, and coastal processes are dominated by waves, surge elevations can reach $O(1)$ m during storms from the south and can result in intense erosion of the coastline (Calliari *et al.*, 1998). Waves are the main hydrodynamic agent with

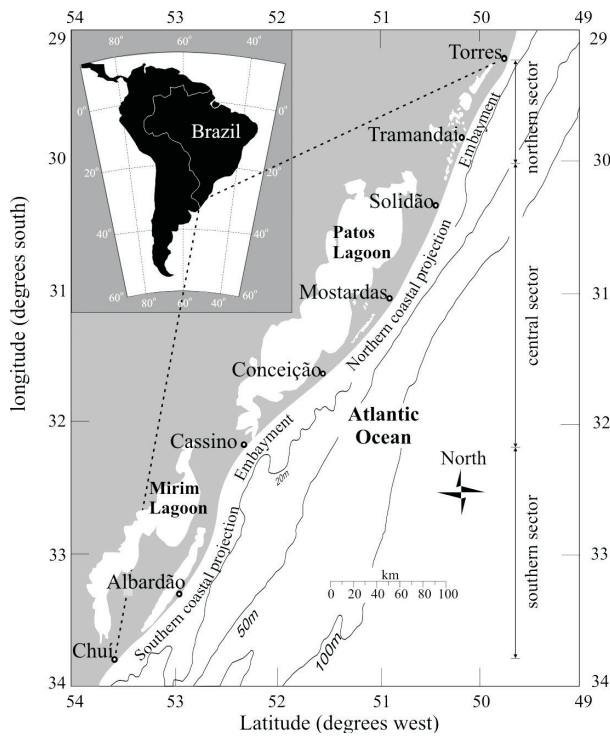


Figure 1 - Location of the study area showing the three major coastal sectors.

mean significant height (H_s) of 1.4 m and peak period (T_p) of 7 s to 9 s that can exceed 3 m and 12 s, respectively, during the passage of extra-tropical cyclones (Almeida & Toldo, 1997).

Three major coastal sectors can be identified (Esteves, 2004): (a) a southern sector, extending 220 km from the Chuí creek at the Uruguayan border to the Patos Lagoon inlet close to Cassino; (b) a central sector extending 275 km north from the Patos Lagoon inlet; and (c) a northern sector extending a further 123 km to the north and bisected by the Tramandaí Lagoon inlet (Figure 1). The average beach slope value (β) is 1/30 along the northern coastal sector (Toldo & Almeida, 2003), varying from 1/26 to 1/40 along the central sector (Barletta, 2000), and from 1/13 to 1/30 along the southern sector (Calliari & Klein, 1993). Typically, nearshore beach slope values below the low waterline (m) are roughly half this value (Gruber et al., 2003). Generally, the RS beaches are composed by well-sorted fine quartzose sands with a mean grain size from 0.15 mm to 0.21 mm (Martins, 1967). Major differences occur in: (1) Estreito, south of the Conceição Lighthouse in the central sector, where the mean grain size varies seasonally from 0.19 mm to 0.27 mm due to the presence of shell fragments (Barletta, 2000); (2) the beaches around the mouth of the Patos Lagoon, where fine sediments from the lagoon reduce the mean size

from 0.135 mm to 0.18 mm (Siegle, 1996); and (3) between Albardão lighthouse and Hermenegildo in the southern sector, where bimodal sediments composed by quartzose fine sands (0.21 mm) and bioclastic gravels (1.5 mm) occur along a 30 km-long segment (Calliari & Klein, 1993). Excluding these areas, analysis of the remaining beach samples reveal a subtle decrease in the mean grain size from south to north along the RS coastline (Esteves, 2004).

Based upon observations of geomorphological features (Tomazelli & Villwock, 1992) it is generally accepted that the net transport of beach sediments along the RS coastline is to the north. These observations are supported by a modeling study of LST by Lima et al. (2001). Owing to trapping by lagoons and other coastal plain environments, little if any fluvial sand has been supplied to the system from inland in the last 5 ka (Tomazelli et al., 1998). The only exceptions are the ephemeral channels that bisect the RS beaches at fairly regular intervals during periods of heavy rainfall. Whilst sometimes causing local erosion $O(10^3 \text{ m}^3)$ (Da Silva et al., 2003), and providing shore-normal sediment supply, their contribution to the net sediment budget is small, at around 3 orders of magnitude less than the annual LST reported by Lima et al. (2001). Single, double and triple offshore bars observed at different locations along the RS coastline are testament to significant cross-shore sediment transport.

Analyses of DGPS survey data for the entire RS shoreline by Esteves (2004) have identified large-scale oscillations in the shoreline position with wavelengths $O(25 \text{ km to } 70 \text{ km})$ and amplitudes $O(40 \text{ m to } 100 \text{ m})$. The scale and location of these features are observed to change alongshore and the loss or gain in beach width at any given location over the short-term is significantly greater than the longer-term changes in shoreline position at that same location. An interesting feature of these oscillations is their ability to develop an almost perfect mirror image over a range of time-scales, i.e. sections of the coast eroding at the some point in time will later accrete (Esteves, 2004).

LST formulae

The most widely used equation to predict LST is the Coastal Engineering Research Center (CERC) formula (Komar & Inman, 1970 in Shore Protection Manual, 1984) which is believed **in ideal conditions** to have an accuracy of ± 30 to 50 percent. In terms of the longshore component of wave energy flux per unit shoreline distance, P , the rate of LST, Q , can be expressed as

$$Q = \frac{K P}{(\rho_s - \rho) g} \quad (1)$$

where K is a coefficient expressing the efficiency of sediment transport (see below), ρ is the water density, ρ_s is the sediment density and g is the acceleration due to gravity. Accurate estimation of the incident wave breaker height $H_{s,b}$ and breaking wave angle relative to the shoreline orientation (θ_b) is of pivotal importance when estimating the LST rate. In the present study we follow methodologies described in the Shore Protection Manual (1984) to derive these parameters.

Eq. 1 is more commonly expressed in units of m^3/s (i.e. the volumetric sediment transport rate) as the CERC formula in the form

$$Q_{CERC} = \frac{K}{16(s-1)(1-p)} \sqrt{\frac{g}{\xi}} H_{s,b}^{2.5} \sin(2\theta_b) \quad (2)$$

where K is the so-called CERC coefficient, s is the specific density of the sediment, p is the sediment porosity and ξ is a wave breaker index, often taken to be 0.78, (Weggel, 1972). Here we calculate K values from the Bailard (1981) equation in the form

$$K = \left[\theta_b, u_{w,b} / w_s = 0.05 + 2.6 \sin^2(2\theta_b) + 0.007(u_{w,b} / w_s) \right] \quad (3)$$

where $u_{w,b}$ is the RMS wave orbital velocity at the breaker point and w_s is the sediment settling velocity defined as

$$w_s = \frac{v}{D_{50}} \left[\left(10.36^2 + 1.049 D_*^3 \right)^{0.5} - 10.36 \right] \quad (4)$$

where D_{50} is the median grain size and the dimensionless grain parameter, D_* is defined as

$$D_* = \left[\frac{g(s-1)}{v^2} \right]^{1/3} D_{50} \quad (5)$$

(Soulsby, 1997) where v is the kinematic viscosity of water. Eq. (3) applies in the range $2.5 \text{ cm/s} < w_s < 20.5 \text{ cm/s}$, $0.2^\circ < \theta_b < 15^\circ$ and $0.3 \text{ m/s} < u_{w,b} < 2.83 \text{ m/s}$. Thus the equation is valid for conditions pertaining along the RS shoreline.

MATERIALS AND METHODS

This study uses data of offshore wave climate data derived by Coli (2000) and data from a Datawell Mk. II Waverider buoy deployed in 15 m water depth approximately for 10 months between October 1996 and

August 1997 at a site located offshore from Cassino (Figure 1). In addition, data related to annual wave directions also come from visual observations of the littoral drift direction at Tramandaí (Nicolodi et al., 2000) and Cassino (Tozzi, 1999) used by Esteves (2004) to define the wave climate scenarios used in the present study for *normal* (i.e. non-ENSO) years and for *La Niña*. Each of the wave scenarios used in the present study are defined in Table 1 which shows H_s values and the number of days and the percentage of time waves from the specified direction approach the RS coastline during a 12-month period. This shows that the wave climate for *normal* years (scenarios 1 & 2) is broken down as follows: (a) NE (45°) and E (90°) waves occur for 62% of the time with $H_s = 0.75 \text{ m}$; (b) S (180°) waves with $H_s = 1.5 \text{ m}$ occur for approximately 16% of the year; (c) waves from the ESE (120°) and SE (135°) occur for between approximately 12% and 22% of the year and have H_s values in the range 0.5 m to 2.0 m; and (d) SSW (215°) storm waves with $H_s = 2.0 \text{ m}$ occur for a maximum of approximately 10% of the time in a given year. In the case of the *La Niña* years (scenarios 3 & 4), there is a reduction in the height and duration of the NE and E waves of 33 % and 8 %, respectively, and a corresponding increase in the duration of waves from the ESE, SE, S and SSW (20 %). However, H_s values for the southerly waves remain the same as that observed in a *normal* year, except the SSW wave that increases from 2.0 m to 2.5 m (Table 1).

The shoreline position measured during April 15th to 17th, 2002 using a kinematic DGPS (Esteves et al., 2003) was used to determine the shoreline orientation angle (θ_s). The survey line was divided into 72 approximately straight-line sections so that the average and maximum change in orientation between any two given sections was only 1.8° and 4.8° , respectively. Values for grain size (here we used available mean grain size, Mz , data) and m used here were obtained from analysis of beach samples and beach profile surveys, respectively, in studies reported by Callari & Klein (1993), Toldo et al. (1993), Barletta (2000) and Gruber et al. (2003), from 15 locations along the RS shoreline. Estimates of Mz , and m for all 72 coastal sections were obtained by cubic spline interpolation.

Changes in shoreline width were estimated using the simple continuity relationship

$$\Delta y = \frac{\Delta Q}{\Delta x(d_b - d_c)} \Delta t \quad (6)$$

where y is alongshore distance, Q is the net alongshore transport in time t , x is cross shore distance, d_b is the berm height and d_c is the depth of closure. Here we simply assume that: (a) along the RS shoreline the

starting width of the beach is 100 m (a typical value for the RS shoreline) and (b) the beach slope and the berm height remain constant with the addition or removal of sediment. The disruption to LST caused by the 4-km long jetties at the entrance of the Patos Lagoon was accounted for by dividing the RS coastline into two regions: a southern region extending from Chuí to the southern Cassino jetty (approximately 220 km); and a central-northern region extending from the northern Cassino jetty to Torres (approximately 400 km). In the simulation, sediment exchanges were not permitted between cells adjacent to the jetties.

Measured changes in the shoreline position were determined every 250 m alongshore using DGPS survey data obtained between the years 1997 (November 26th to 28th), 1998 (November 17th to 19th), 1999 (November 10th to 11th and 19th), 2000 (June 26th to 28th) and 2002 (April 15th to 17th) by Esteves (2004) using the ArcView extension Digital Shoreline Analysis System 2.0 (DSAS 2.0), developed by the U.S. Geological Survey (Thieler et al., 2003). These data are used to assess changes in shoreline position predicted by the simple approach outlined above for the different wave scenarios defined in Table 1.

RESULTS AND DISCUSSION

Net annual LST

Using the CERC formula for the scenarios described in Table 1, Figure 2 shows Q_{net} values computed using the CERC formula for wave climate scenarios 1 to 4 (Table 1). Positive and negative Q_{tot} values express longshore transport towards the NE and SW, respectively. Here typical Q_{net} values are $O(0.05 \times 10^6)$ m³/year, with maximum Q_{net} values $O(0.2 \times 10^6)$ m³/year. Considering scenario 1 where $\theta_{SE} = 120^\circ$, Figure 2a shows that Q_{net} along the RS shoreline is relatively small and is directed to the north when $H_s < 1.0$ m. For $H_s > 1.0$ m, Figure 2a shows both a reversal in the direction of LST to the south along certain stretches of the coastline and a further enhancement of LST towards the north along others, leading to divergence points for sediment transport. These occur around

Albardão, Cassino, Solidão and south of Torres. Figure 2a shows also that for the larger waves, net LST is directed towards the south in the area between Cassino and Mostardas. In this way the sediment eroded from areas further north (i.e. the Conceição lighthouse area) might be partly balancing the sediment deficit caused by the obstruction of LST south of the 4-km long jetties. Progressively adding SSW waves to scenario 1 (Figures 2b to 2d), there is a reduction in extent of the areas showing net transport to the south. For SE waves of $H_s = 1.5$ m, more than 10 days of SSW waves are required to reverse LST to the north along the whole shoreline. For SE waves of $H_s = 2.0$ m, at least 30 days of SSW waves are required to redirect LST northwards.

A rather different result is obtained for scenario 2 (Figure 2e to 2h) where the simulation includes only a relatively small change in the direction of the SE waves from 120° to 135° . This change is sufficient to suppress the tendency for LST to proceed southwards and, except a small amount of LST to the south around the area of Conceição, all the littoral drift is directed to the north. As the number of days waves approach the coastline from the SSW is increased, the magnitude of Q_{net} along most of the shoreline declines except from Cassino to Mostardas. This is attributable to the corresponding reduction in the time waves approach from the SE (135°) direction. For most coastal locations, this wave direction optimizes LST, thus a reduction in the occurrence of these waves has a significant impact on Q_{net} values. It is clear also that as H_s for SE waves is increased, LST is increasingly directed northwards so that the magnitude of Q_{net} along the whole shoreline for $H_s = 2.0$ m is almost a mirror image of that for $H_s = 0.5$ m. We see strong evidence of differences in the magnitude of Q_{net} that may result in regions of beach erosion and accretion. In the case of scenario 2, divergence of LST occurs only at the Conceição area (a recognized area of erosion), although we also see significant changes in the magnitude of Q_{net} at Albardão and Cassino.

Comments made above for scenario 2 apply equally to scenarios 3 & 4 (Figure 2i to 2p). Both show that in nearly all cases, net LST is directed to the north.

Table 1. Wave scenarios used to estimate the LST for the RS coastline

θ_{wave}	Scenario 1			Scenario 2			Scenario 3			Scenario 4		
	H_s	days	% of time									
45	0.75	113	31.0	0.75	113	31.0	0.5	84	23.0	0.5	84	23.0
90	0.75	113	31.0	0.75	113	31.0	0.5	84	23.0	0.5	84	23.0
120	0.5 to 2.0	44 to 79	12.1 to 21.6				0.5 to 2.0	64 to 99	17.5 to 27.2			
135				0.5 to 2.0	44 to 79	12.1 to 21.6				0.5 to 2.0	64 to 99	17.5 to 27.2
180	1.5	60	16.4	1.5	60	16.4	1.5	83	22.7	1.5	83	22.7
215	2.0	0 to 35	0 to 9.6	2.0	0 to 35	0 to 9.6	2.5	15 to 50	4.1 to 13.8	2.5	15 to 50	4.1 to 13.8

However, unlike scenario 2, these cases show a significant increase in Q_{net} values in response to increases in the number of SSW wave days, except for SE waves of $H_s = 2$ m south of Cassino and north of Mostardas. This is attributable to a reduction in the duration of waves from NE and E directions thereby reducing the contribution to Q_{net} values made by LST travelling to the south. In general terms, trends in Q_{net} values for scenarios 3 and 4 look very similar to the trends for scenarios 1 & 2. However, in the *La Niña* cases, the northward transport of sediment along the whole RS shoreline is enhanced and differences between Q_{net} values for adjacent coastal sectors are larger than in *normal* years. It might be anticipated therefore that erosion and accretion rates may be accelerated during

La Niña years. Evidence to support this is presented by Esteves (2004).

Changes in the morphology of the RS shoreline

We turn attention now to consider the predicted changes in the width of the RS shoreline attributable to the net import or export of sediment by LST between adjacent coastal segments. For brevity here we only show results from scenarios 1 and 2 in Figure 3. The upper panels show the coastal orientation for the southern and central-northern sectors. Directly below these are two sets of graphs depicting the changes in beach width predicted from the model. The first is for SE waves where $\theta_w = 120^\circ$ and the second is for SE waves where $\theta_w = 135^\circ$. In both cases the simulations

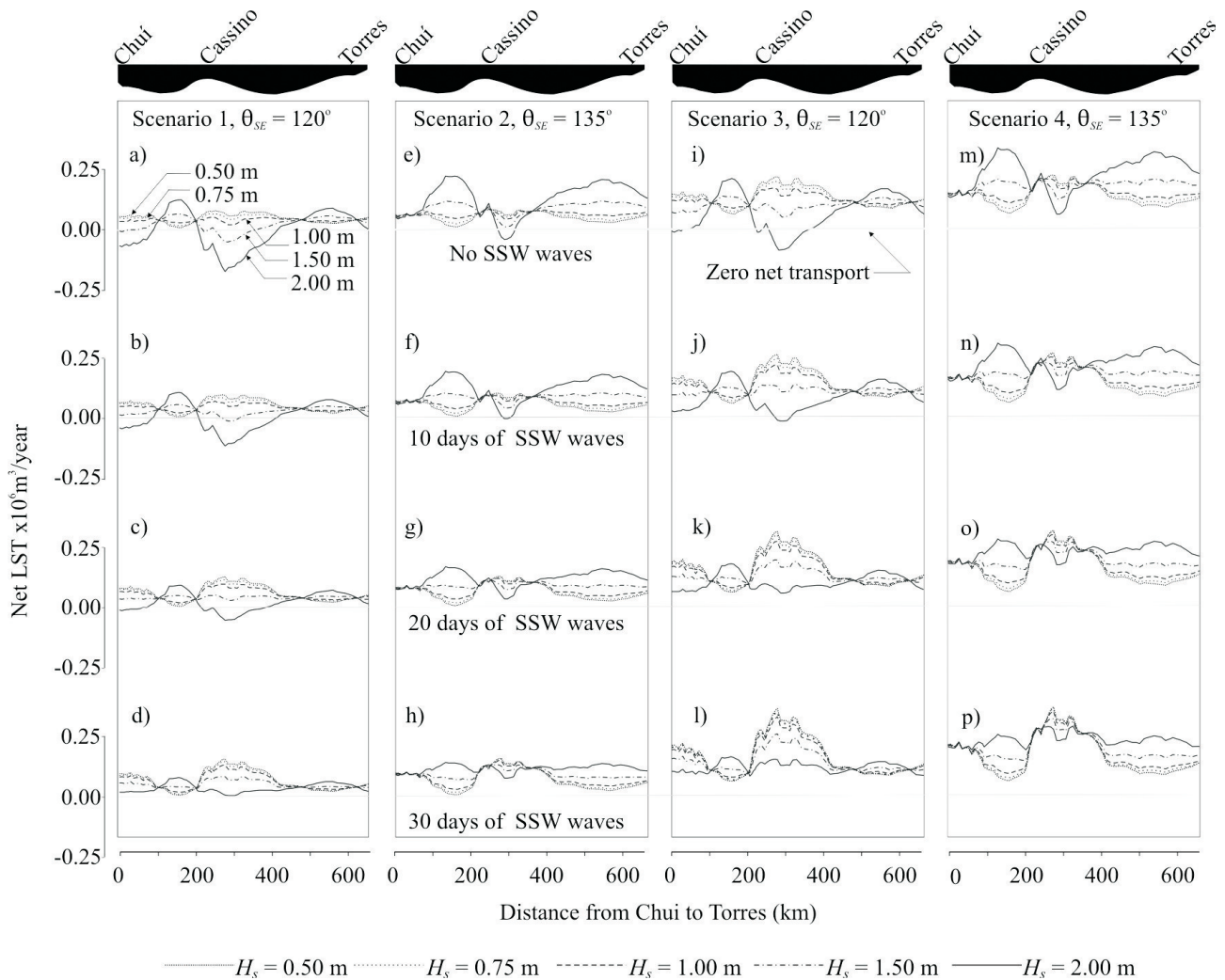


Figure 2 - Net annual rates of LST predicted for the RS coastline by the CERC formula for wave scenarios 1 to 4 with SE waves from 120° (scenarios 1 and 3) and from 135° (scenarios 2 and 4) and SSW waves from 215° for (a) 0 days; (b) 10 days; (c) 20 days; and (d) 30 days. Positive values represent northward LST and negative values represent southward LST. Each wave scenario is defined in Table 1.

encompass SE waves with $H_s = 0.5$ m, 1.0 m and 2.0 m, and waves from the SSW ($\theta_w = 220^\circ$) are considered occurring for 40 days together with waves from other directions as defined in Table 1. Shading is used on these plots to help show clearly regions of the RS coastline experiencing net erosion or accretion as defined by predicted changes in the width of the beach.

In the case of scenario 1, Figure 3a shows that for SE waves with $H_s = 0.5$ m opposite trends in erosion and accretion to those normally expected are found. We see accretion along the southern shorelines of the coastal projections, some erosion in the embayment around Cassino and maximum changes in beach width $O(5$ m). This is caused by the dominance of waves from the NE and E, which drive LST southwards along the northern shorelines of the coastal projections. A significant decrease in the efficiency of these waves to transport sediments along the southern shores of the coastal projections results in accretion. This southerly drift of sediment is reversed in the case of SE waves with $H_s = 1.0$ m, resulting in very little change in the beach width with the whole shoreline being approximately static. Increasing SE wave height further to $H_s = 2.0$ m gives rise to erosion along the southern shorelines of the coastal projections and accretion in the embayments in the manner normally observed along the RS shoreline. In this case maximum changes in beach width are $O(15$ m). In addition, subtle changes in coastal orientation give rise to wave-like rhythmic

modulation of the shoreline position along certain stretches of the coastline. Patterns similar in frequency to these are also evident in the DGPS survey data for the RS shoreline reported by Esteves (2004). These are discussed further below. Although not illustrated here, it is noted that the effect of reducing the number of SSW wave days to 10 tends to increase the magnitude of shoreline changes along the RS shoreline by a factor of 2. This is attributable to SSW waves transporting sediment northwards and thus reversing the tendency of the SE waves to move sediment southwards when $\theta_s < 30^\circ$.

For scenario 2, Figure 3b shows trends similar to those found for scenario 1 in cases of SE waves ($\theta_w = 135^\circ$) with $H_s = 0.5$ m and 1.0 m. The only major difference is a tendency for greater erosion to occur immediately south of Torres due to the local coastal orientation relative to this wave climate. SE waves with $H_s = 2.0$ m result in different magnitudes of erosion and accretion to those predicted in the case of scenario 1. In particular we note much greater erosion along the southern shore of the northern coastal projection and accretion in the embayment south of Torres. In this case, even more extensive rhythmic oscillation of the shoreline position are observed along stretches of the coastline with amplitudes typically $O(10$ m) and wavelengths $O(25$ km) in the southern region and $O(75$ km) in the central-northern region. These values agree well with observations reported by Esteves (2004) and are mainly

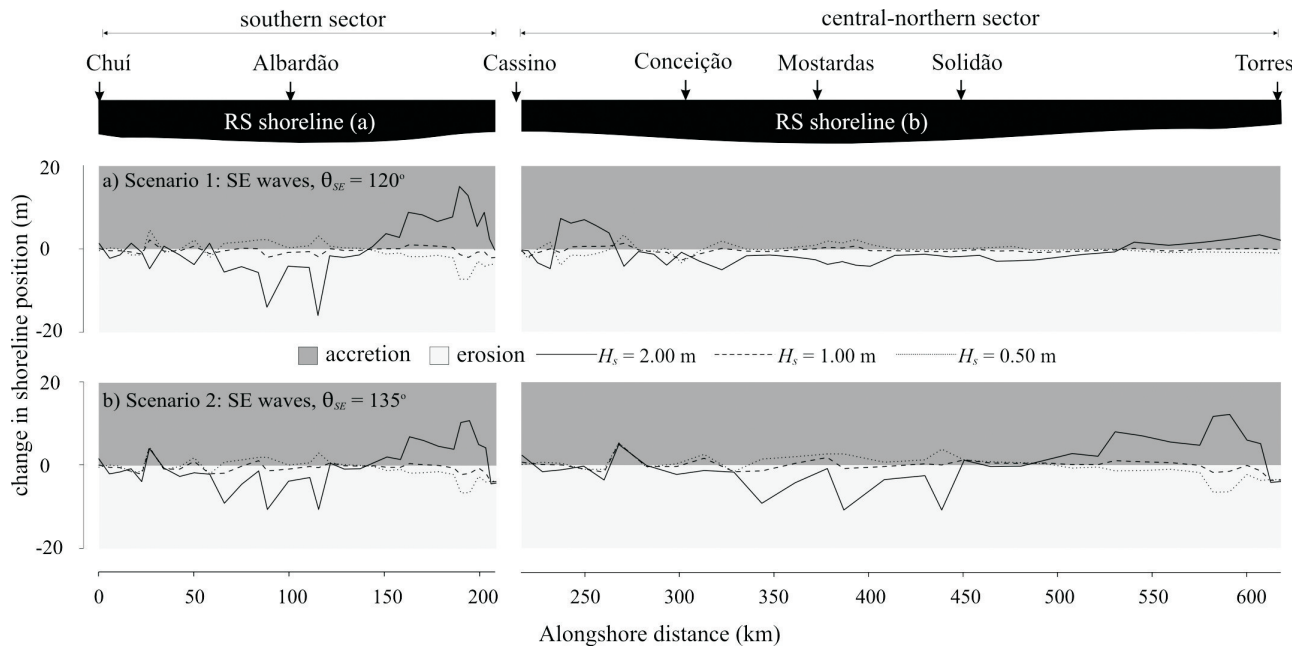


Figure 3 - Simulation of changes in shoreline morphology showing shoreline orientation and the predicted change in the beach width for the southern and northern coastal sections for: a) scenario 1; and b) Scenario 2. Each wave scenario is defined in Table 1, (Note: in these simulations SSW waves are present for 40 days in the year).

attributed to subtle changes in coastline orientation and in the grain size.

A further observation concerns the balance between the net gains and losses of beach material along the whole RS shoreline. Considering separately the area enclosed by lines for SE waves with $H_s = 2.0$ m above (accretion) and below (erosion) zero change in shoreline position in Figure 3, reveals that net losses and gains are approximately in balance within the RS coast. The simulations show that the source of sediments for accretion in the embayment areas are primarily the coastal projections and thus no net import of sediment to the RS coastline is required to maintain the observed present day patterns of change. Thus, despite the large annual predicted LST rates, results for scenarios 1 and 2 show that for the majority of the shoreline, the combined effect of a 'typical' wave climate (i.e. waves defined in Table 1 and SE waves with $H_s = 1.0$) results in only small net annual changes in the beach width.

To illustrate clearly the alternate zones of erosion and accretion along the RS shoreline and their response to shifts in the wave climate, locations subject to erosion or accretion (defined by predicted annual changes in the width of the shoreline) for wave scenarios 1 to 4 (Table 1) and for SE waves of heights 0.5 m, 1.0 m and 2.0 m from 120° and 135° are shown in Figure 4. Light and darker shading on each of the horizontal bars is used to indicate erosion or accretion, respectively. Figure 4 reveals a complex alternate pattern of erosion and accretion zones and shows that quite subtle

changes in the wave climate can have a profound effect on the local behaviour of the shoreline. For example, in scenario 1, a change in the height of the SE waves reverses the mode of coastline change for long stretches of the coastline so that areas subject to accretion when $H_s = 0.5$ m, become areas of erosion when $H_s = 1.0$ m. These changes are even more distinct for $H_s = 2.0$ m. Figure 4 shows also that only a small change of 15° to the direction of the SE waves from $\theta_o = 120^\circ$ to $\theta_o = 135^\circ$ results in the opposite trend with zones of erosion becoming zones of accretion along long stretches of the coastline. Similar trends can be seen for the other wave scenarios examined here.

A feature of Figure 4 is the regularity of erosion and accretion zones along some stretches of the coastline (e.g. scenario 4, $H_s = 2.0$ m). Figure 4 may help to explain therefore the rhythmic patterns of alternate shoreline erosion and accretion that reverses in consecutive years revealed by the analysis of DGPS survey data by Esteves (2004). These observations are not unique as similar pattern of changes are also reported by List et al. (2003) for the coastlines of the Outer Banks (North Carolina, USA) and Cape Cod (Massachusetts, USA). Figure 4 suggests that a shift in the annual dominance of one or more wave directions and/or changes of the wave height or period can reverse any tendency of erosion or accretion for a given section of coastline. If these changes occur on an approximately annual time-scale (as available wave and meteorological data suggest), it is possible that this mechanism could produce a mirror image of the shoreline position between

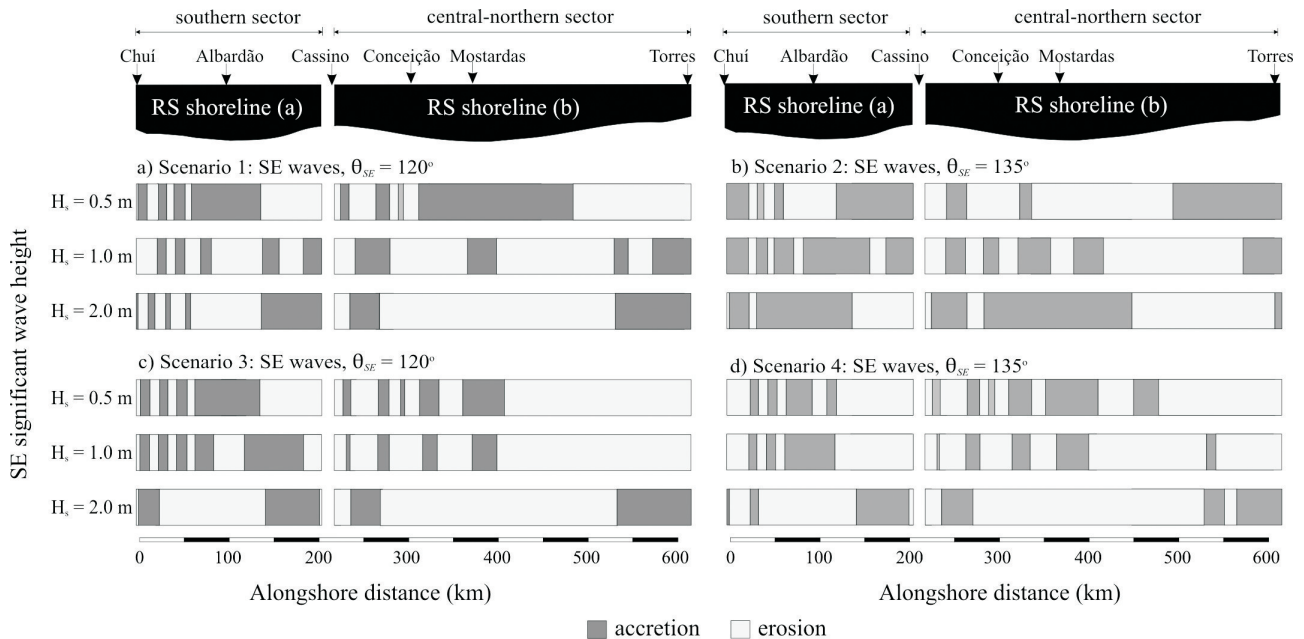


Figure 4 - Locations along the RS coast subject to erosion or accretion defined by predicted annual changes in the width of the shoreline for wave scenarios 1 to 4 (Table 1) for SE waves of heights 0.50 m, 1.00 m and 2.00 m.

consecutive years. It is unlikely that changes in the wave climate alone are sufficient to produce all the changes along the RS shoreline measured by the DGPS surveys. Here it is speculated that mechanisms leading to the enhancement of shoreline perturbations by LST when the angle between the wave crests and the general shoreline orientation is higher than the angle of maximum sediment transport (e.g. Murray & Ashton, 2003) may also play a role in the formation and modulation of these rhythmic shoreline features. This combination of mechanism requires further study.

SUMMARY AND CONCLUSIONS

In *normal* years Q_{net} values are $O(0.2 \times 10^6) \text{ m}^3/\text{year}$ and can exceed $O(1.0 \times 10^6) \text{ m}^3/\text{year}$ in the case of ENSO events. The balance between erosion and accretion is perturbed during ENSO events and can reverse normal tendency of shoreline changes. Therefore small changes to the present-day wave climate along the RS shoreline could impact significantly upon rates of LST. In a '*normal*' year, the typical combination of wave heights and directions results in relatively small net change in shoreline position. Areas of erosion are found to be coincident with the coastal projections with accretion largely confined to the embayments. The rhythmic annual and seasonal oscillations in shoreline position measured by DGPS surveys are also evident in the modelling results indicating that the mechanisms forcing changes in the shoreline position are primarily linked to the wave climate and coastline orientation during a given period of time. The ability of the simple modelling approaches used here to reproduce approximately the observed behaviour of the shoreline indicates that this approach may also be a useful tool with which to investigate the likely shoreline changes resulting from changes in the future wave climate. At the very least it will aid identification of areas potentially at risk from severe erosion in the future and thereby assist in aspects of coastal management.

REFERENCES

- Almeida, L.E.S.B. & Toldo Jr., E.E. 1997. Estudos Ambientais em Áreas Costeiras e Oceânicas na Região Sul do País – Região de Osório, RS. Instituto de Pesquisas Hidráulicas, UFRGS (Porto Alegre, Brazil), Relatório Técnico, 110p.
- Bailard, J.A. 1981. An energetics total load sediment transport model for a plane sloping beach. J. Geoph. Res. 86: 10938-10954.
- Barletta, R.C. 2000. Efeitos da interação oceano-atmosfera sobre a morfodinâmica das praias do litoral central do Rio Grande do Sul, Brasil. Dissertação de Mestrado, FURG (Rio Grande, Brasil). 160p.
- Calliari, L.J. & Klein, A.H.F. 1993. Características morfodinâmicas e sedimentológicas das praias oceânicas entre Rio Grande e Chuí, RS. Pesquisas. 20(1): 48-56.
- Calliari, L.J.; Tozzi, H.A.M. & Klein, A.H.F. 1998. Beach morphology and coastline erosion associated with storm surges in southern Brazil-Rio Grande to Chuí. An. Acad. Bras. Cienc. 70(2): 231-247.
- Coli, A.B. 2000. Estudo sobre o clima de ondas em Rio Grande, RS (Brasil). Dissertação de Mestrado, FURG (Rio Grande, Brazil). 80p.
- Da Silva R.P.; Calliari, L.J. & Tozzi, H.A.M. 2003. The influence of washouts on the erosive susceptibility of the Rio Grande do Sul coastline between Cassino and Chui beaches, southern Brazil. J. Coast. Res. SI 35: 332-338.
- Esteves, L.S.; Dillenburg, S.R. & Toldo Jr., E.E. 2003. Regional alongshore variability of shoreline movements in southern Brazil. CD of Proceedings Coastal Sediments'03 (Clearwater Beach, Florida). Regional alongshore variability of shoreline movements.pdf. 11p.
- Esteves, L.S. 2004. Variabilidade espaço-temporal dos deslocamentos da linha de costa no Rio Grande do Sul. Tese de Doutorado, Instituto de Geociências, UFRGS (Porto Alegre, Brasil). 139p.
- Gruber, N.L.S.; Toldo Jr., E.E.; Barboza, E.G. & Nicolodi, J.L. 2003. Equilibrium beach and shoreface profile of the Rio Grande do Sul coast - south Brazil. J. Coast. Res. SI 35: 253-259.
- Komar, P.D. & Inman, D.L. 1970. Longshore sand transport on beaches. J. Geoph. Res. 75(30): 5514-5527.
- Lima, S.F.; Almeida, L.E.S.B. & Toldo Jr., E.E. 2001. Estimativa da capacidade do transporte longitudinal de sedimentos a partir de dados de ondas papa a costa do Rio Grande do Sul. Pesquisas. 28(2): 99-107.
- List, J.H.; Farris, A.S. & Sullivan, C. 2003. Large-scale response of foreshore slope to storms events. Cd of Proceedings Coastal Sediments'03 (Clearwater Beach, Florida). Large-scale response of foreshore slope to storms events.pdf. 14p.
- Martins, L.R. 1967. Aspectos deposicionais e texturais dos sedimentos praias e eólicos da Planície Costeira do Rio Grande do Sul. Publicação Especial da Escola de Geologia, UFRGS, (Porto Alegre, Brasil). 13: 102p.
- Murray, A.B. & Ashton, A. 2003. Sandy-coastline evolution as an example of pattern formation involving emergent structures and interactions. Cd of Proceedings Coastal Sediments'03 (Clearwater

- Beach, Florida). Sandy-coastline evolution as an example of pattern.pdf. 12p.
- Nicolodi, J.L.; Toldo Jr., E.E. & Gruber, N.L.S. 2000. Análise da direcionalidade das correntes litorâneas no litoral norte do Rio Grande do Sul. Anais da XIII Semana Nacional de Oceanografia (Itajaí, Brasil). I: 461-463.
- Shore Protection Manual (4th Ed.). 1984. U.S. Army Engineer Waterways Experiment Station, U.S. Government Printing Office, Washington, DC.
- Siegle, E. 1996. Distribuição dos sedimentos litorâneos entre o farol da Conceição e farol do Chuí, RS, e fatores condicionantes. Trabalho de Graduação, FURG (Rio Grande, Brasil). 91p.
- Soulsby, R.L. 1997. Dynamics of marine sands: a manual for practical applications, Thomas Telford Publications, London. 249p.
- Thieler, E.R.; Martin, D. & Ergul, A. 2003. The digital shoreline analysis system, version 2.0: shoreline change measurement software extension for Arcview. USGS open-file report 03-076.
- Toldo Jr., E.E. & Almeida, L.E.S.B. 2003. A linha d'água como posição indicadora da linha de praia. CD of Proceedings, IX Congresso da ABEQUA (Recife, Brasil). 88.pdf. 3p.
- Toldo Jr., E.E.; Dillenburg, S.R.; Almeida, L.E.S.B.; Tabajara, L.L.; Martins, R.R. & Cunha, L.O.B.P. 1993. Parâmetros morfodinâmicos da praia de Imbé, RS. Pesquisas, 20(1):27-32.
- Tomazelli, L.J. & Villwock, J.A. 1992. Considerações sobre o ambiente praial e a deriva litorânea de sedimentos ao longo do litoral norte do Rio Grande do Sul, Brasil. Pesquisas. 19: 3-12.
- Tomazelli, L.J.; Villwock, J.A.; Dillenburg, S.R.; Bachi, F.A. & Dehnardt, B.A. 1998. Significance of present-day coastal erosion and marine transgression, Rio Grande do Sul, southern Brazil. An. Acad. Bras. Cienc. 70(2): 221-229.
- Tozzi, H.A.M. 1999. Influência das tempestades extratropicais sobre o estoque subaéreo das praias entre Rio Grande e Chuí, RS. Campanha de outono e inverno de 1996. Dissertação de Mestrado, UFRGS (Porto Alegre, Brasil). 115p.
- Weggel, J.R. 1972. Maximum breaker height. J. Water. Ports Coast. Eng. Div. Vol. 98, No. WW4, 529-548.